

STOCHASTIC RELIABILITY IN CONTACT PROBLEMS FOR COMPOSITES WITH SPHERICAL PARTICLES

MARCIN KAMIŃSKI

Division of Mechanics of Materials, Technical University of Łódź

e-mail: marcin@kmm-ix.p.lodz.pl

The application of the stochastic perturbation technique in the classical Hertz contact problem of a composite with spherical particle is presented in the paper. The perturbation approach is used in conjunction with the Weibull-Second Order Third Moment (W-SOTM) reliability model in numerical analysis of the composite. All computational experiments are carried out using symbolic computation package MAPLE, that makes it possible to visualize the deterministic sensitivity gradients as well as to show probabilistic moments of contact stresses. The entire methodology can be applied to analytical solutions of contact problems with a more complicated contact surface geometry and, on the other hand, to computational implementation in the Finite or Boundary Element Method programs for simulations of some contact phenomena.

Key words: reliability analysis, contact problems, composite materials, stochastic perturbation method

1. Introduction

Usually, contact problems are formulated for homogeneous bodies, but in general, they are very important for composites as well. Contact stresses can be analyzed in the case of composites reinforced with spherical particles and particles with a more general shape such as ellipsoidal or paraboloidal one, for instance. Moreover, contact problems in composites can be analyzed to simulate delamination effects or interface defects between various components in the laminates and fiber-reinforced composites. As it can be expected, contact stresses depend on interrelations between material properties of the contacting composite components. The analysis is definitely more complicated in the case of a randomly defined material and/or geometrical parameters – not only the

expected values, but also higher order probabilistic moments can be decisive for the final results of the contact problem.

At the same time, significant progress is being observed in the field of stochastic mechanics (see Grigoriu, 2000). Probabilistic numerical experiments with Monte-Carlo simulation (MCS) (see Kamiński, 2001; Kleiber and Hien, 1992) and with Stochastic Finite Element Method (SFEM) (see Kleiber and Hien, 1992; Liu et al., 1986) prove that usually the second order perturbation analysis is exact enough, while the second probabilistic moment approach is not satisfactory, considering the fact that in most cases the third order (skewness) parameters differ from 0. Additionally, the stochastic perturbation method gives essential computation time savings in comparison with the MCS technique and the stochastic spectral modeling (see Ghanem and Spanos, 1992, 1997). Furthermore, even if a Gaussian random variable is very precisely digitally simulated, the third order probabilistic moments and coefficients slightly differ from 0. That is why, the Second Order Third Moment (SOTM) stochastic analysis is proposed below, in addition to the reliability study of contact problems based on the Weibull probability density function (PDF). It should be underlined that the Weibull probability density function is frequently used in probabilistic analysis of fracture phenomena in homogeneous structures and composites (see Beyerlein and Phoenix, 1997; Lund, 1998).

On the other hand, it is known that the reliability analysis has been modeled using the First Order Reliability Method (FORM) and the Second Order Reliability Method (SORM) (see Brandt et al., 1984; Ghanem and Spanos, 1992). These approaches do not enable one to include the influence of the third order probabilistic characteristics, necessary for the Weibull statistics, and that is why the Third Order Reliability Method (TORM) is proposed on the basis of the SOTM stochastic perturbation method.

To illustrate the entire approach, the stochastic perturbation reliability analysis of a linear elastic contact is carried out for a composite reinforced with spherical particles. Since the solution for the deterministic problem is known and has been worked out analytically, the probabilistic analysis is made using symbolic computations package MAPLE (see Char et al., 1992). Computations of the reliability limit function and probabilistic moments of the contact stresses as well as some numerical sensitivity studies together with visualization of all computed functions are carried out by the use of this package. This methodology can be successfully applied to randomization of all contact problems in reliability studies, where contact stresses are described by the closed form equations. Otherwise, computational implementations of the Stochastic Finite (see Buczkowski and Kleiber, 1999) or Boundary Element

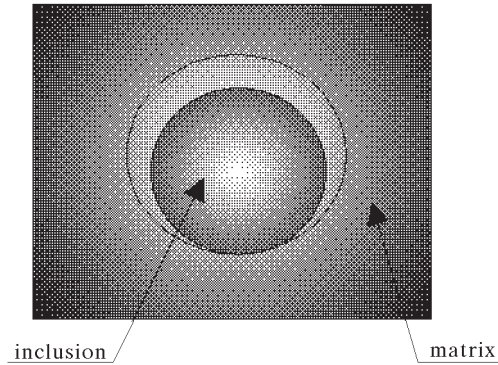


Fig. 2. 3D cross-section view of particle-reinforced composite

where r denotes the distance between the points M , N and the symmetry axis introduced at C . If the composite components are loaded by the vertical force P acting along the vertical axis at the point C , then some local strains are induced in the neighborhood of this point. They are a result of the contact phenomenon on a small circular surface (contact area). Assuming that the radii R_1 and R_2 of the composite constituents are sufficiently greater than the radius of the contact area, then the results of the Bussinesq problem of a linear elastic halfspace loaded by a concentrated force can be adopted here (see Timoshenko and Goodier, 1951). For this purpose let us denote by w_1 the vertical displacement induced by the local vertical strain of the point M belonging to the matrix; and by w_2 – the corresponding displacement of the point N in the vertical direction. Finally, assuming that the tangential plane at the point C remains unmovable during local compression, the close-up of the two points M and N can be expressed by some real η as

$$\eta = \alpha - (w_1 + w_2) = \frac{r^2(R_1 - R_2)}{2R_1R_2} \quad (2.2)$$

If M and N belong to the contact area, their displacements w_i for $i = 1, 2$ can be written as (see Timoshenko and Goodier, 1951)

$$w_i = \frac{1 - \nu_i^2}{\pi E_i} \iint q \, ds d\varphi \quad (2.3)$$

which follows the symmetry of the pressure intensity q and the corresponding local strains with respect to the vertical axis at the point C . The integration is carried out over the entire contact surface, therefore

$$(k_1 + k_2) \iint q \, ds d\varphi = \alpha - \frac{r^2(R_1 - R_2)}{2R_1R_2} \quad (2.4)$$

where k_1 and k_2 can be obtained from Eq. (2.3). Now, we are looking for such an expression for q , so that the above equation could be fulfilled. It can be obtained for the pressure distribution on the contact surface represented by the coordinates of a hemisphere with the radius a constructed on that surface. If q_0 is taken as the pressure at the point C , then one can show that

$$\int q \, ds = \frac{q_0}{a} A \tag{2.5}$$

where

$$A = \frac{\pi}{a} (a^2 - r^2 \sin^2 \varphi) \tag{2.6}$$

what gives

$$\frac{\pi(k_1 + k_2)q_0}{a} \int_0^{\frac{\pi}{2}} (a^2 - r^2 \sin^2 \varphi) \, d\varphi = \alpha - \frac{r^2(R_1 - R_2)}{2R_1R_2} \tag{2.7}$$

Finally, the parameters a and α can be found as

$$a = \sqrt[3]{\frac{3\pi P(k_1 + k_2)R_1R_2}{4(R_1 - R_2)}} \tag{2.8}$$

$$\alpha = \sqrt[3]{\frac{9\pi^2 P^2(k_1 + k_2)^2(R_1 - R_2)}{16R_1R_2}}$$

which gives the maximal pressure on the contact surface

$$q = \frac{3P}{2\pi a^2} \tag{2.9}$$

Then, the normal stress can be defined as

$$\sigma_z = - \int_0^a 3qr \, dr \, z^3(r^2 + z^2)^{-\frac{5}{2}} = q \left[-1 + z^3(a^2 + z^2)^{\frac{3}{2}} \right] \tag{2.10}$$

Let us note that the shear stresses are equal to 0, which results from the spherical symmetry of the reinforcing particle, however in the case of ellipsoidal reinforcement the shear stresses differ from 0 (see Timoshenko and Goodier, 1951).

The main purpose of further analysis is to determine probabilistic characteristics of the maximal contact stresses as well as contact surface geometrical

parameters. Since the spherical particle surrounding the matrix is considered, let us assume that the difference $R_1 - R_2$ is smaller than R_2 .

This parameter is treated as the input design parameter in further sensitivity analysis. The characteristics mentioned above are necessary in final stochastic reliability computations and, considering complexity of equations describing the reliability parameters, the second order stochastic perturbation method is proposed.

3. Stochastic perturbation approach

Let \mathcal{H} be some Hilbert's space defined on the domain \mathcal{D} with the real values set \mathcal{R} . Let (Ω, σ, P) denote the probability space, $\mathbf{x} \in \mathcal{D}$ and $\theta \in \Omega$, while $\Theta : \Omega \rightarrow \mathcal{R}$. Let us consider the differential operator $L(\mathbf{x}; \theta)$ defined on the product $\mathcal{H} \times \Theta$, whose coefficients exhibit random fluctuations with respect to some independent variables. The random coefficients of the differential operator are restricted to be second order random processes. Then, we illustrate the stochastic second order third central probabilistic moment approach using a solution to the following equation

$$L(\mathbf{x}; \omega)u(\mathbf{x}; \omega) = f(\mathbf{x}; \omega) \quad (3.1)$$

being a mathematical description of a physical problem. The random response of the system is denoted here by $u(\mathbf{x}; \omega)$, while its admissible excitation by $f(\mathbf{x}; \omega)$.

As it is known, analytical solutions to such a class of partial differential equations are available for some specific cases only, and that is why a general method of extending such solutions would be very powerful. Various mathematical methods can be proposed here, some of them are listed by Ghanem and Spanos (1997), Kleiber and Hien (1992), however, in this paper, the second order perturbation third central probabilistic moment approach is applied (see Peng et al., 1998). The second order perturbation follows a traditional approach in this area (and the lack of convergence studies with respect to the Taylor expansion order). The third probabilistic moment method reflects the need of modeling of unsymmetric random variables.

Let us denote for this purpose the vector of input random fields by $\{b^r(\mathbf{x}; \omega)\}$ and its probability density by $p(b^r)$ and $p(b^r, b^s)$ respectively, where $r, s = 1, 2, \dots, R$ are indices of the random variables. Then, the expect-

ted value of b^r is defined as

$$E[b^r] = \int_{-\infty}^{+\infty} b^r p(b^r) db^r \tag{3.2}$$

and the covariance as

$$\text{Cov}(b^r, b^s) = \int_{-\infty}^{+\infty} \int_{-\infty}^{+\infty} (b^r - E[b^r])(b^s - E[b^s]) p(b^r, b^s) db^r db^s \tag{3.3}$$

Next, the skewness parameter $S(u_i)$ is calculated

$$S(u) = \frac{1}{\sigma^3(u)} \int_{-\infty}^{+\infty} (u - E[u])^3 p_R(b) db \tag{3.4}$$

In further applications, the Weibull distribution is used with the probability density function defined as

$$p_R = \begin{cases} \frac{\beta}{\lambda} \left(\frac{x - \bar{x}}{\lambda}\right)^{\beta-1} \exp\left[-\left(\frac{x - \bar{x}}{\lambda}\right)^\beta\right] & \text{for } x > \bar{x} \\ 0 & \text{for } x < \bar{x} \end{cases} \tag{3.5}$$

where

- β - Weibull shape parameter
- λ - scale parameter
- \bar{x} - location parameter, which indicates the smallest value of the random variable \mathbf{x} for which the probability density function is positive.

Considering this definition, the Weibull PDF is used for general mechanical applications, where many random variables must be nonnegative (Young’s modulus, some geometrical parameters, for instance) and especially in composites failure and fatigue modeling (see Beyerlein and Phoenix, 1997). Let us note that if a discrete representation of the random variable $b(\mathbf{x}; \theta)$ is used, then statistical estimators can be applied to approximate probabilistic moments of this variable of any order.

Afterwards, all material and physical parameters of Ω and all state functions being random fields are represented by the use of the stochastic second order expansion via the Taylor series as follows

$$F(b(\mathbf{x}; \theta); \mathbf{x}) = F^0(b^0(\mathbf{x}; \theta); \mathbf{x}) + \varepsilon F^{,rs}(b(\mathbf{x}; \theta); \mathbf{x}) \Delta b^r + \frac{\varepsilon^2}{2} F^{,rs}(b(\mathbf{x}; \theta); \mathbf{x}) \Delta b^r \Delta b^s \tag{3.6}$$

where ε is a given small perturbation, $\varepsilon \Delta b^r$ denotes the first order variation of Δb^r about its expected value $E[b^r]$ and $F^{(n)}(b(\mathbf{x}; \theta); \mathbf{x})$ represents the n th order partial derivatives with respect to the random variables, while $F^{(n)}(b^0(\mathbf{x}; \theta); \mathbf{x})$ denotes the n th order partial derivative calculated at the expected value of the input random variables vector. Let us note that the second order equation is obtained here by multiplying the R -variate probability density function $p_R(b_1, b_2, \dots, b_R)$ by the ε^2 -terms and integrating over the random field domain $\mathbf{b}(\mathbf{x}; \theta)$.

Applying the stochastic second order Taylor expansion to Eq. (3.1) and equating terms of the same order for $\varepsilon = 1$ yields:

— 0th order equations

$$L^0(b^0(\mathbf{x}; \theta); \mathbf{x})u^0(b^0(\mathbf{x}; \theta); \mathbf{x}) = f^0(b^0(\mathbf{x}; \theta); \mathbf{x}) \tag{3.7}$$

— 1st order equations (for $r = 1, \dots, R$)

$$L^0(b^0(\mathbf{x}; \theta); \mathbf{x})u^{,r}(b^0(\mathbf{x}; \theta); \mathbf{x}) = f^{,r}(b^0(\mathbf{x}; \theta); \mathbf{x}) - L^{,r}(b^0(\mathbf{x}; \theta); \mathbf{x})u^0(b^0(\mathbf{x}; \theta); \mathbf{x}) \tag{3.8}$$

— 2nd order equations (for $r, s = 1, \dots, R$)

$$L^0(b^0(\mathbf{x}; \theta); \mathbf{x})u^{(2)}(b^0(\mathbf{x}; \theta); \mathbf{x}) = \left\{ f^{,rs}(b^0(\mathbf{x}; \theta); \mathbf{x}) - L^{,rs}(b^0(\mathbf{x}; \theta); \mathbf{x})u^0(b^0(\mathbf{x}; \theta); \mathbf{x}) + 2L^{,r}(b^0(\mathbf{x}; \theta); \mathbf{x})u^{,s}(b^0(\mathbf{x}; \theta); \mathbf{x}) \right\} \text{Cov}(b^r, b^s) \tag{3.9}$$

Equation (3.7) is solved for u^0 to obtain the probabilistic solution for the considered equilibrium problem, then Eq. (3.8) – for first order terms of $u^{,r}$ and, finally, Eq. (3.9) – for $u^{(2)}$. The two probabilistic moment characterization of all the state functions for the boundary value problem starts from the expected value of the stress tensor components. Using definition (3.2) and substituting the second order expansion it can be found (see Kleiber and Hien, 1992), that

$$E[u[\mathbf{b}(\mathbf{x}; \theta); \mathbf{x}]] = u^0[\mathbf{b}(\mathbf{x}; \theta); \mathbf{x}] + \frac{1}{2}u^{,rs}[\mathbf{b}(\mathbf{x}; \theta); \mathbf{x}]S_b^{,rs} \tag{3.10}$$

Next, the first order cross-covariances for the solution components are derived as follows (see Kamiński, 2001; Kleiber and Hien, 1992)

$$\begin{aligned} \text{Cov} \left(u[\mathbf{b}(\mathbf{x}^{(1)}; \theta); \mathbf{x}^{(1)}]; u[\mathbf{b}(\mathbf{x}^{(2)}; \theta); \mathbf{x}^{(2)}] \right) &= S_u(\mathbf{x}^{(1)}; \mathbf{x}^{(2)}) = \\ &= \int_{-\infty}^{+\infty} \left\{ u[\mathbf{b}(\mathbf{x}^{(1)}; \theta); \mathbf{x}^{(1)}] - E[u[\mathbf{b}(\mathbf{x}^{(1)}; \theta); \mathbf{x}^{(1)}]] \right\} \cdot \\ &\cdot \left\{ u[\mathbf{b}(\mathbf{x}^{(2)}; \theta); \mathbf{x}^{(2)}] - E[u[\mathbf{b}(\mathbf{x}^{(2)}; \theta); \mathbf{x}^{(2)}]] \right\} p_R(\mathbf{b}(\mathbf{x}; \theta)) \, d\mathbf{b} \end{aligned} \tag{3.11}$$

which gives

$$S_u(\mathbf{x}^{(1)}; \mathbf{x}^{(2)}; \theta) = u^r(\mathbf{x}^{(1)}; \theta)u^s(\mathbf{x}^{(2)}; \theta)S_b^{rs}(\mathbf{x}^{(1)}; \mathbf{x}^{(2)}; \theta) \tag{3.12}$$

Analogously, the third order probabilistic moments can be derived in the stochastic second order perturbation approach.

4. Weibull-Second Order Third Moment reliability approach

Starting from the moments and the stochastic perturbation methodology presented in the previous section, we compute the first three probabilistic characteristics of the vertical stresses $E[\sigma_z(x; \omega)]$, $\text{var}(\sigma_z(x; \omega))$ and $S(\sigma_z(x; \omega))$ as follows (see Timoshenko and Goodier, 1951)

$$E[\sigma_z] = \sigma_z^0 + \frac{1}{2} \sum_{i=1}^n \frac{\partial^2 \sigma_z}{\partial b_i^2} \sigma^2(b_i) \tag{4.1}$$

$$\begin{aligned} \sigma^2(\sigma_z) &= \sigma_z^2 + \sum_{i=1}^n \left[\left(\frac{\partial \sigma_z}{\partial b_i} \right)^2 + \sigma_z \frac{\partial^2 \sigma_z}{\partial b_i^2} \right] \sigma^2(b_i) + \\ &+ \sum_{i=1}^n \frac{\partial \sigma_z}{\partial b_i} \frac{\partial^2 \sigma_z}{\partial b_i^2} S(b_i) \sigma^3(b_i) - E^2[\sigma_z] \end{aligned}$$

and

$$\begin{aligned} S(\sigma_z) &= \left\{ \sigma_z^3 + \frac{3}{2} \sum_{i=1}^n \left[2\sigma_z \left(\frac{\partial \sigma_z}{\partial b_i} \right)^2 + \sigma_z^2 \frac{\partial^2 \sigma_z}{\partial b_i^2} \right] \sigma^2(b_i) + \right. \\ &+ \sum_{i=1}^n \left[\left(\frac{\partial \sigma_z}{\partial b_i} \right)^3 + 3\sigma_z \frac{\partial \sigma_z}{\partial b_i} \frac{\partial^2 \sigma_z}{\partial b_i^2} \right] S(b_i) \sigma^3(b_i) - \\ &\left. - E^3[\sigma_z] - 3E[\sigma_z] \sigma^2(\sigma_z) \right\} \frac{1}{\sigma^3(\sigma_z)} \end{aligned} \tag{4.2}$$

Having computed the first three probabilistic moments of contact stresses (expected values, standard deviations and skewness coefficients), the random field of the limit function $g(z; \omega)$ is to be proposed. Usually, it can be introduced as the difference between the allowable and actual stresses $\sigma_z(z; \omega)$ induced in the composite

$$g(z; \omega) = \sigma_{all}(\omega) - \sigma_z(z; \omega) \tag{4.3}$$

Let us underline that the allowable stresses are most frequently analyzed as random variables in the interior of statistically homogeneous materials, whereas the actual stresses are random fields. That is why the computational analysis is carried out in Section 5.3 for a specific value of the vertical coordinate z . The random variable of the allowable stresses $\sigma_{all}(\omega)$ is specified by the use of the first three probabilistic moments $E[\sigma_{all}(\omega)]$, $\text{var}(\sigma_{all}(\omega))$ and $S(\sigma_{all}(\omega))$. Then, the corresponding probabilistic characteristics of the limit function are calculated as

$$E[g] = g^0 + \frac{1}{2} \sum_{i=1}^n \frac{\partial^2 g}{\partial b_i^2} \sigma^2(b_i) \quad (4.4)$$

$$\begin{aligned} \sigma^2(g) &= (g^0)^2 + \sum_{i=1}^n \left[\left(\frac{\partial g}{\partial b_i} \right)^2 + g^0 \frac{\partial^2 g}{\partial b_i^2} \right] \sigma^2(b_i) + \\ &+ \sum_{i=1}^n \frac{\partial g}{\partial b_i} \frac{\partial^2 g}{\partial b_i^2} S(b_i) \sigma^3(b_i) - E^2[g] \end{aligned}$$

and

$$\begin{aligned} S(g) &= \left\{ (g^0)^3 + \frac{3}{2} \sum_{i=1}^n \left[2g^0 \left(\frac{\partial g}{\partial b_i} \right)^2 + (g^0)^2 \frac{\partial^2 g}{\partial b_i^2} \right] \sigma^2(b_i) + \right. \\ &+ \sum_{i=1}^n \left[\left(\frac{\partial g}{\partial b_i} \right)^3 + 3g^0 \frac{\partial g}{\partial b_i} \frac{\partial^2 g}{\partial b_i^2} \right] S(b_i) \sigma^3(b_i) - \\ &\left. - E^3[g] - 3E[g] \sigma^2(g) \right\} \frac{1}{\sigma^3(g)} \end{aligned} \quad (4.5)$$

By inserting the limit state function g from Eq. (4.3) into Eqs (4.4) and (4.5) and assuming that the random variable of the allowable stresses and the random field of the actual stresses are uncorrelated, one obtains

$$E[g] = \sigma_{all}^0 - \sigma_z^0 - \frac{1}{2} \sum_{i=1}^n \frac{\partial^2 \sigma_z}{\partial b_i^2} \sigma^2(b_i) \quad (4.6)$$

$$\begin{aligned} \sigma^2(g) &= (\sigma_{all}^0 - \sigma_z^0)^2 + \sum_{i=1}^n \left[\left(\frac{\partial \sigma_z}{\partial b_i} \right)^2 - (\sigma_{all}^0 - \sigma_z^0) \frac{\partial^2 \sigma_z}{\partial b_i^2} \right] \sigma^2(b_i) + \\ &+ \sum_{i=1}^n \frac{\partial \sigma_z}{\partial b_i} \frac{\partial^2 \sigma_z}{\partial b_i^2} S(b_i) \sigma^3(b_i) - E^2[\sigma_{all} - \sigma_z] \end{aligned}$$

and

$$\begin{aligned}
 S(g) = & \left\{ (\sigma_{all}^0 - \sigma_z^0)^3 + \frac{3}{2} \sum_{i=1}^n \left[2(\sigma_{all}^0 \sigma_z^0) \left(\frac{\partial \sigma_z}{\partial b_i} \right)^2 + (\sigma_{all}^0 - \sigma_z^0)^2 \frac{\partial^2 \sigma_z}{\partial b_i^2} \right] \sigma^2(b_i) + \right. \\
 & + \sum_{i=1}^n \left[\left(\frac{\partial g}{\partial b_i} \right)^3 + 3g^0 \frac{\partial g}{\partial b_i} \frac{\partial^2 g}{\partial b_i^2} \right] S(b_i) \sigma^3(b_i) - \\
 & \left. - E^3[\sigma_{all}^0 - \sigma_z^0] - 3E[\sigma_{all}^0 - \sigma_z^0] \sigma^2(\sigma_{all}^0 - \sigma_z^0) \right\} \frac{1}{\sigma^3(\sigma_{all}^0 - \sigma_z^0)}
 \end{aligned} \tag{4.7}$$

Comparing the second order second moment (SOSM) approach with the second order third moment (SOTM) approach, it is seen that the expected values are described by exactly the same equation, while the standard deviations (or variances) have some extra components resulting from the skewness of the analyzed PDF; the third order parameter of the output PDF is taken into account in the SOTM-based analysis, only.

Finally, the parameters $x(g)$, $\lambda(g)$ and $\beta(g)$ of the equivalent Weibull PDF are derived from the following system of equations

$$\begin{aligned}
 E[g] &= \lambda(g) \Gamma\left(1 + \frac{1}{\beta(g)}\right) + x(g) \\
 \sigma^2(g) &= \lambda^2(g) \left[\Gamma\left(1 + \frac{2}{\beta(g)}\right) - \Gamma^2\left(1 + \frac{1}{\beta(g)}\right) \right] \\
 S(g) &= \lambda^3(g) \left[\Gamma\left(1 + \frac{3}{\beta(g)}\right) - 3\Gamma\left(1 + \frac{2}{\beta(g)}\right) \Gamma\left(1 + \frac{1}{\beta(g)}\right) \right] \frac{1}{\sigma^2(g)} \\
 &+ 2\Gamma^3\left(1 + \frac{1}{\beta(g)}\right) \frac{1}{\sigma^2(g)}
 \end{aligned} \tag{4.8}$$

where the Gamma function is defined as

$$\Gamma(x) = \begin{cases} \int_0^\infty e^{-t} t^{x-1} dt & \text{for } x > 0 \\ \lim_{n \rightarrow \infty} \frac{n! n^{x-1}}{x(x+1)(x+2)\dots(x+n-1)} & \text{for } x \in \mathcal{R} \end{cases} \tag{4.9}$$

It should be mentioned that approach based on the symbolic computations is the most efficient method of solving these equations and of computing probabilistic parameters of the equivalent Weibull distribution. Finally, the structural reliability index R of the limit function g is calculated from the following formula

$$R(g) = \exp\left[-\left(-\frac{x(g)}{\beta(g)}\right)^{\lambda(g)}\right] \tag{4.10}$$

Values of this index should behave like the classical probability index, i.e. be greater or equal to 0 and less or equal to 1.

5. Computational experiments

Computational experiments are conducted by the use of system MAPLE for symbolic computations (see Char et al., 1992), where the stochastic second order perturbation method in W-SOTM reliability analysis of contact problems has been implemented. The entire analysis is divided into three groups of essentially various numerical examples:

1. Deterministic analysis and sensitivity study (see Haug et al., 1986) of a contact problem with respect to the vertical spatial coordinate
2. Numerical modeling by randomizing most of the input parameters based on the stochastic second order perturbation
3. Stochastic reliability modeling according to the Weibull Second Order Third Moment approach (see Peng et al., 1998).

5.1. Example 1: Deterministic sensitivity of contact problem in a composite

Deterministic analysis and sensitivity of contact stresses in a two component composite with spherical particles is verified with respect to the vertical spatial coordinate. The following data are adopted for the computational analysis: $E_2 = 2.0 \cdot 10^9$, $\nu_1 = 0.3$, $\nu_2 = 0.2$, $R_2 = 0.18$, $P = 10.0 \cdot 10^5$, $\alpha = E_1/E_2 = 2.0$, $\beta = R_1/R_2 = 1.001 - 1.01$.

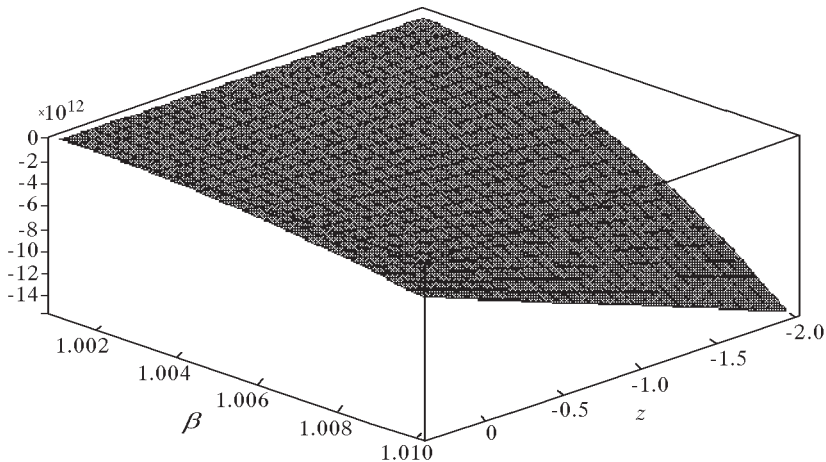


Fig. 3. Contact stresses in the spherical particle-reinforced composite

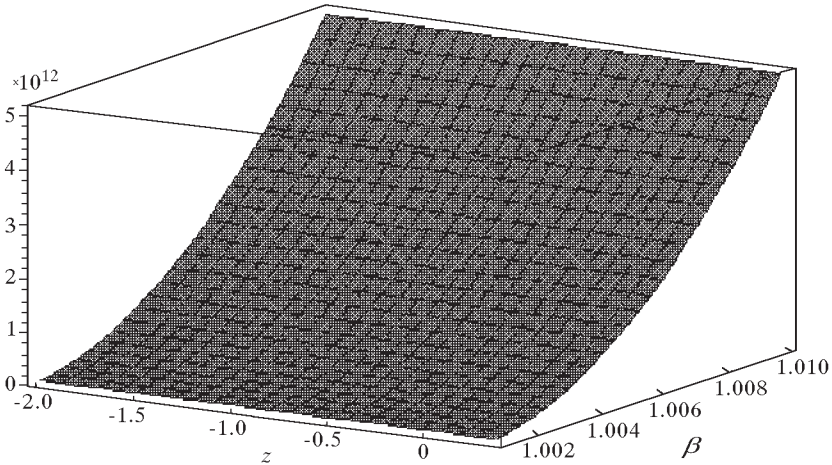


Fig. 4. Sensitivity of contact stresses to vertical spatial coordinate z

The computational analysis of the vertical contact stresses and their sensitivity gradients $d\sigma_z/dz$ with respect to the spatial coordinate is presented in Fig. 3 and Fig. 4, this coordinate and the radii ratio β are marked on the vertical axes of these figures. We observe that the compressive contact stresses are most sensitive to the parameter β for its value tending to ∞ (progressive separation of the reinforcing particle from the surrounding matrix). Moreover, it is visible that the results is quite nonsensitive with respect to the vertical coordinate z what cannot be predicted from the definition of σ_z , cf Eq. (2.10). One of the main benefits flowing from making use of the package MAPLE is visualization of variations of the stresses and their sensitivity gradients, which can be studied in these figures.

5.2. Example 2: Stochastic modeling of the contact phenomenon

All the input parameters of the analyzed contact problem are now treated as random variables: Young's moduli and Poisson's ratios of the composite components as well as their radii. The deterministically calculated vertical stresses in the contact area are compared below with the expected values, standard deviations and probabilistic envelope values of the vertical contact stresses for $z = 0.018$ and $z = -0.5$. The standard deviations of the variables are taken in the range of 10% of the corresponding expectations; all variables are assumed to be uncorrelated.

The computed deterministic contact stresses are shown in Fig. 5, Fig. 9,

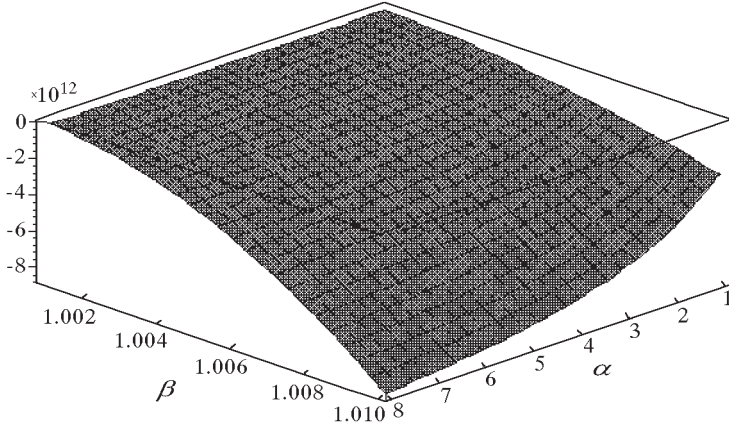


Fig. 5. Deterministic contact stresses; $z = 0.018$

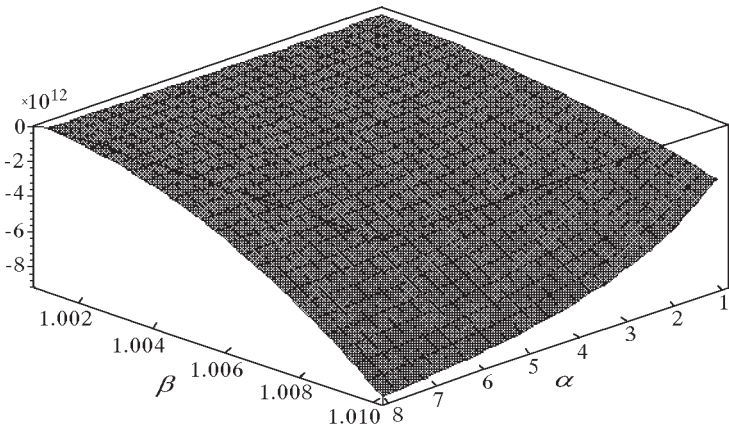


Fig. 6. Expected values of contact stresses; $z = 0.018$

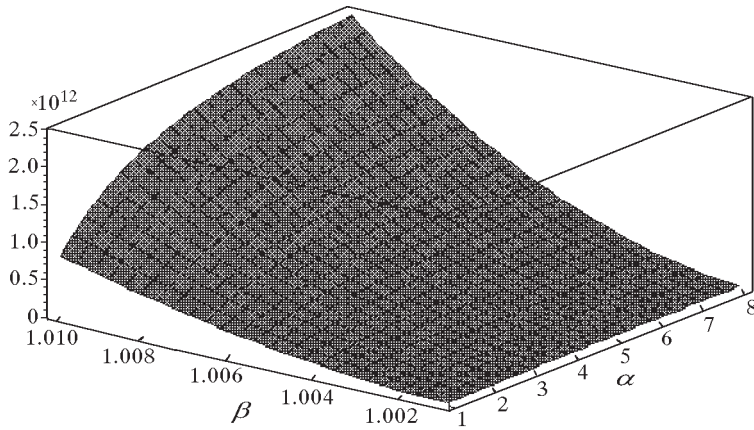


Fig. 7. Standard deviations of contact stresses; $z = 0.018$

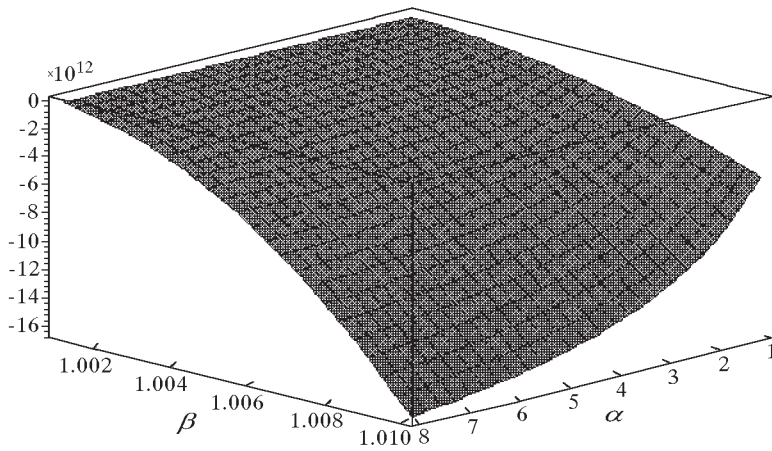


Fig. 8. Probabilistic envelope of contact stresses; $z = 0.018$

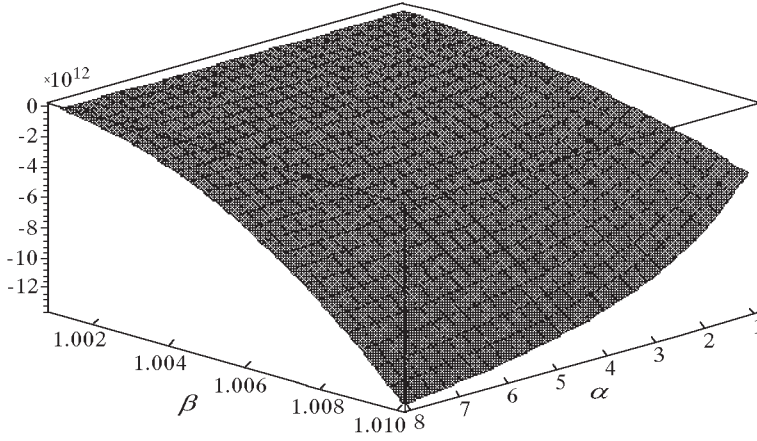


Fig. 9. Deterministic contact stresses; $z = -0.5$

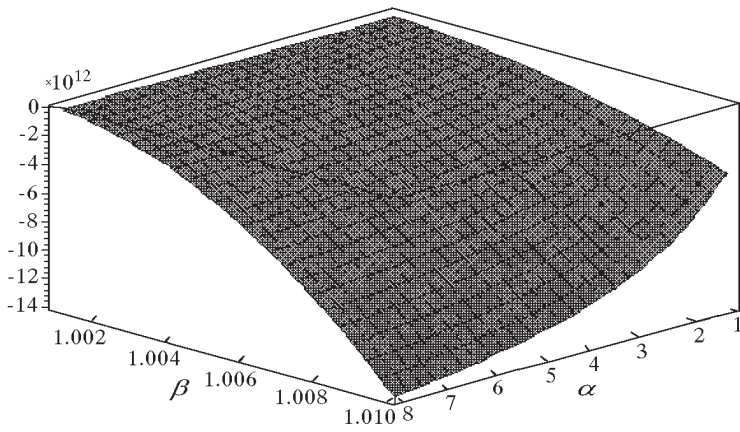


Fig. 10. Expected values of contact stresses; $z = -0.5$

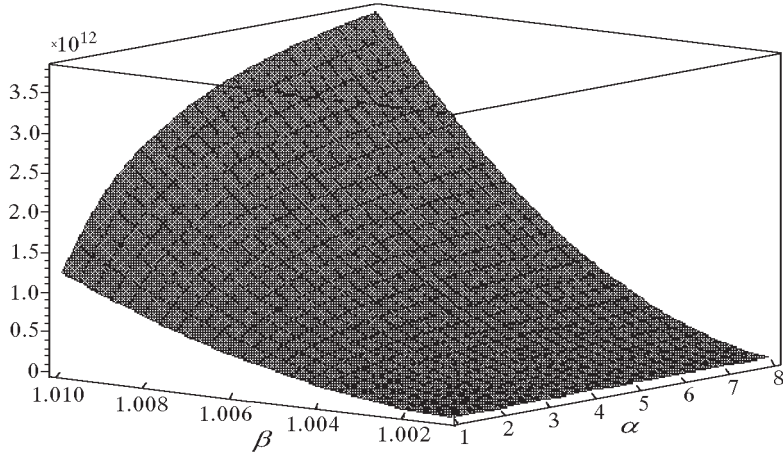


Fig. 11. Standard deviations of contact stresses; $z = -0.5$

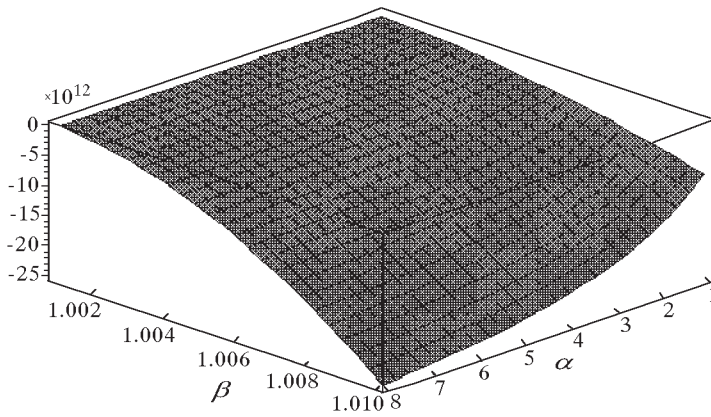


Fig. 12. Probabilistic envelope of contact stresses; $z = -0.5$

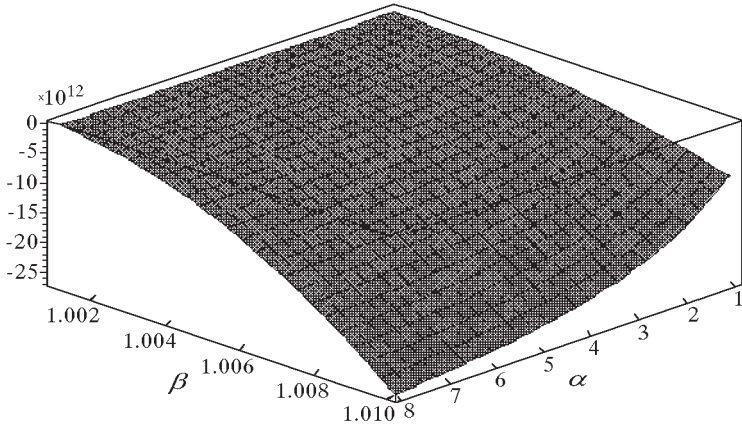


Fig. 13. Deterministic contact stresses; $z = -2.0$

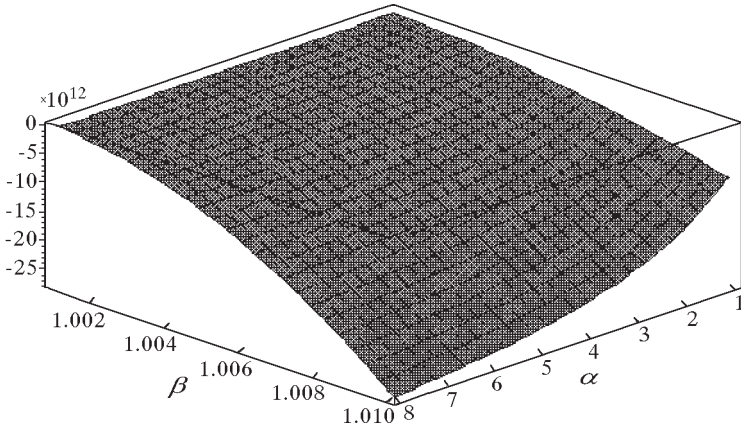


Fig. 14. Expected values of contact stresses; $z = -2.0$

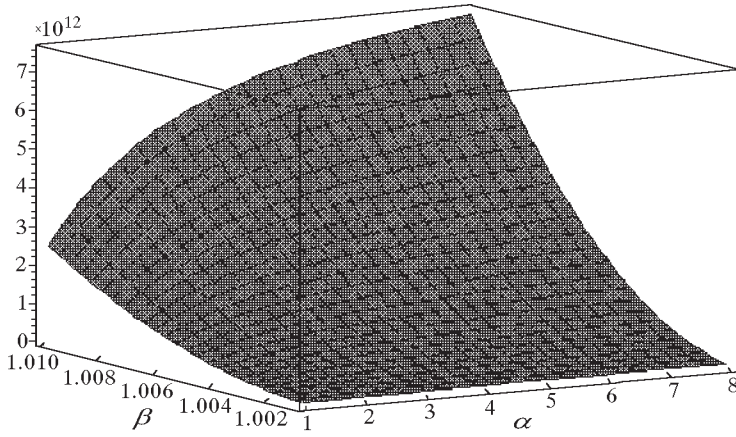


Fig. 15. Standard deviations of contact stresses; $z = -2.0$

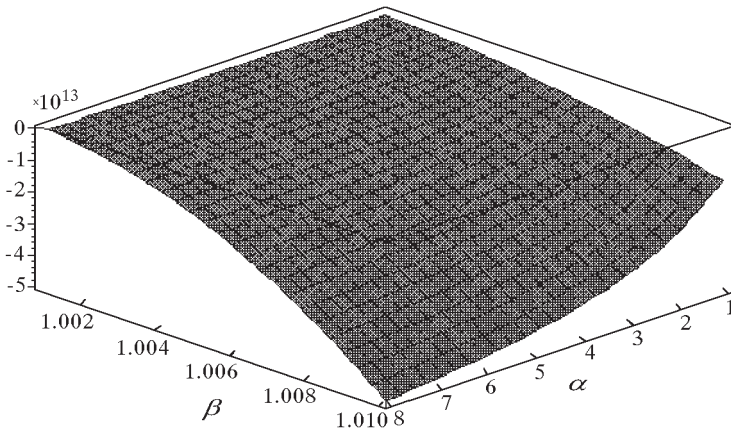


Fig. 16. Probabilistic envelope of contact stresses; $z = -2.0$

Fig. 13 for the particle center $z = 0.018$, for some point belonging to the matrix $z = -0.5$ and $z = -2.0$, respectively. The expected values of the contact stresses are shown in Fig. 6, Fig. 10, Fig. 14 for the same points, the standard deviations are shown in Fig. 7, Fig. 11, Fig. 15, while the probabilistic envelopes for the surfaces of these stresses are presented in Fig. 8, Fig. 12 and Fig. 16. The vertical contact stresses are marked on the vertical axes; the horizontal axes define the reinforcement ratio of the composite α and the ratio between the particle and the surrounding matrix radii β . All the surfaces shown in these figures have the same character and variability with respect to the input parameters α and β , apart from the standard deviations plots.

Analyzing Figures 5, 6, 9, 10, 13 and 14, it can be seen that the expected values of the contact stress surfaces are quite close to those obtained from the corresponding deterministic analyses. Essential differences are observed between Figures 5-8, 9-12 and 13-16, where the probabilistic envelopes of these stresses are shown. These envelopes are determined for a particular z on the basis of the results presented in Figures 6, 7, 10, 11, 14 and 15 as

$$\text{Env}(f(z); z) = E[f(z); z] - 3\sigma(f(z); z) \quad (5.1)$$

Let us note that Eq. (5.1) is frequently used in Stochastic Finite Element computations and stochastic fatigue analysis (see Liu et al., 1986). The values of the probabilistic envelope surfaces are significantly smaller than the corresponding values obtained from deterministic analysis, which means that the computational analysis based on the stochastic perturbation is more restrictive than that of the classical model. The same concerns the corresponding expected values. All the surfaces combined in the probability envelope show that the vertical stresses tend to 0 for the reinforcement ratio approaching 1 and the matrix assuming the radius of the spherical particle. Comparing the deterministic and stochastic results, one can clearly see that the contact stresses are most sensitive to the vertical spatial coordinate.

Analyzing Figures 5-8, 10-12 and 14-16 in terms of variations of the contact stresses with respect to the composite reinforcement ratio, it is observed that the greatest sensitivity appears for $\alpha \rightarrow 1$, which means that the greatest variations of the examined probabilistic stresses are obtained for the homogeneous contact problem. The sensitivity analysis requires further numerical examinations aimed at interrelations between Poisson's ratios of both composite components.

5.3. Example 3: Reliability analysis for the particle reinforced composite

The computational study on structural reliability, proposed in the the-

oretical considerations, is the main subject of the next example. The set of input data together with their probabilistic characteristics is given in Table 1 for the same composite contact problem as before. The Weibull probability density function (PDF) of the limit function is determined together with its probabilistic moments of up to 3rd order (cf Table 1) obtained from symbolic computational solution to nonlinear equations system (4.8).

Table 1. Probabilistic input data for reliability index computations

Parameter	Value
E_2	$2.0 \cdot 10^6$
ν_1	0.3
ν_2	0.2
R_2	1.8
P	$5.0 \cdot 10^2$
z	-0.018
$\sigma(E_2)$	$0.2 \cdot 10^6$
$S(E_2)$	0.0
$\sigma(R_2)$	0.018
$S(R_2)$	0.0
σ_{all}	$-4.0 \cdot 10^5$
$\alpha(\sigma_{all})$	10.0
$\beta(\sigma_{all})$	1.01
$E[g]$	-211378.33
$\sigma(g)$	38213.61838 ($\alpha = 0.18$)
$S(g)$	5.158577

First, it can be seen that even for a relatively small input coefficient of variation of the input parameters (not greater than 0.1), the randomness level of the output function is about 18% of the relevant expected value. That is why the proposed third moment approach is more accurate for the analyzed contact problem. Furthermore, we observe that even for the input skewnesses equal to 0, the corresponding third order probabilistic characteristics differ from 0, which reflects the differences in algebraic combinations of characteristics of lower order, cf Eq. (4.7). In further analysis it is necessary to verify

the sensitivity (both in the deterministic and stochastic context, see Haug et al. (1986), Kleiber and Hien (1992)) of the output Weibull PDF probabilistic moments with respect to all input mechanical and geometrical parameters and their random characteristics. At the same time, the cross-correlation function of the contact stresses $\text{Cov}(\sigma(z_1), \sigma(z_2))$ can be symbolically computed using the program MAPLE.

6. Conclusions

- The above presented analysis reveals various sources of randomness and stochasticity in contact problems of the spherical particle reinforced composites. In comparison to the second order second probabilistic moment approach, third order probabilistic moments of both input and output parameters are analyzed. It is demonstrated that even for the skewnesses of the inputs equal to 0, the output third order probabilistic moments in reliability studies slightly differ from 0. It results from the main idea of the SOTM approach and from the interrelations between probabilistic characteristics of the lower order. Furthermore, it is observed that the deterministic values of the state functions are quite close to the computed expected values. They are considerably greater and well approximated by their probabilistic envelopes, which confirms the usefulness of these envelopes in various stochastic numerical experiments.
- The most interesting extension of this study would be introducing:
 - randomness of non-spherical (ellipsoidal) contact surface
 - more realistic incremental Stochastic Finite or Boundary Element Method (SFEM, see Kamiński (2001), Kleiber and Hien, (1992) or SBEM, see Burczyński (1995), respectively) analysis of nonlinear geometry of the contacting surface, see Buczkowski and Kleiber (1999).
- Application of the computational W-SOTM reliability study to various numerical analyses of composites would be interesting, too. Neglecting the relatively simple character of the deterministic contact problem, the geometrical sensitivity of the contact stresses values is decisive for this analysis, both in the deterministic and stochastic cases. Considering the above, one can conclude that the stochastic second order perturbation analysis in conjunction with mathematical symbolic computations is a

powerful stochastic computational tool. However, the limitations on the input randomness level, typical for such an analysis, must be fulfilled.

References

1. BEYERLEIN I.J., PHOENIX S.L., 1997, Statistics of Fracture for an Elastic Notched Composite Lamina Containing Weibull Fibers, *Engng. Fract. Mech.*, **57**, 2/3, 267-299
2. BRANDT A., JENDO S., MARKS W., 1984, Probabilistic Approach to Reliability-Based Optimum Structural Design, *Engng. Trans.*, **32**, 1, 57-74
3. BUCZKOWSKI R., KLEIBER M., 1999, A Stochastic Model of Rough Surfaces for Finite Element Contact Analysis, *Comput. Meth. Appl. Mech. Engng.*, **169**, 43-59
4. BURCZYŃSKI T., 1995, *Boundary Element Method in Mechanics* (in Polish), WNT, Warsaw
5. CHAR B.W., GEDDES K.O., GONNET G.H., LEONG B.L., MONAGAN M.B., WATT S.M., 1992, *First Leaves: A Tutorial Introduction to Maple V*, Springer-Verlag
6. FISH J., EDIT., 1999, Computational Advances in Modeling Composites and Heterogeneous Materials, *Comput. Meth. Appl. Mech. Engng.*, **172**
7. GHANEM R.G., SPANOS P.D., 1997, Spectral Techniques for Stochastic Finite Elements, *Arch. Comput. Meth. Engng.*, **4**, 1, 63-100
8. GHANEM R.G., SPANOS P.D., 1992, Spectral Stochastic Finite-Element Formulation for Reliability Analysis, *J. Engng. Mech. ASCE*, **117**, 10, 2351-2372
9. GRIGORIU M., 2000, Stochastic Mechanics, *Int. J. Sol. Struct.*, **37**, 197-214
10. HAUG E.J., CHOI K.K., KOMKOV V., 1986, *Design Sensitivity Analysis of Structural Systems*, Ser. Math. Sci. Engng., Academic Press
11. KAMIŃSKI M., 2001, Stochastic Second Order Perturbation Approach to the Stress-Based Finite Element Method, *Int. J. Sol. Struct.*, **38**, 21, 3831-3852
12. KLEIBER M., HIEN T.D., 1992, *Stochastic Finite Element Method*, Wiley
13. LIU W.K., BELYTSCHKO T., MANI A., 1986, Probabilistic Finite Elements for Nonlinear Structural Dynamics, *Comput. Meth. Appl. Mech. Engng.*, **56**, 61-81
14. LUND E., 1998, Shape Optimization Using Weibull Statistics of Brittle Failure, *Struct. Optimiz.*, **15**, 208-214

15. PENG X.Q., GENG L., LIYAN W., LIU G.R., YAM K.Y., 1998, A Stochastic Finite Element Method for Fatigue Reliability Analysis of Gear Teeth Subjected to Bending, *Comput. Mech.*, **21**, 253-261
16. TIMOSHENKO S., GOODIER S.N., 1951, *Theory of Elasticity*, McGraw-Hill, Inc.

Stochastyczna analiza niezawodności w zagadnieniu kontaktowym kompozytu ze sferycznymi inkluzjami

Streszczenie

Tematem niniejszej pracy jest zastosowanie stochastycznej metody perturbacji w analizie niezawodności materiałów kompozytowych ze sferycznymi inkluzjami. W analizie tej wykorzystano stochastyczną metodę perturbacji drugiego rzędu uwzględniając momenty probabilistyczne rzędu trzeciego. Zastosowane podejście umożliwiło potraktowanie wybranych parametrów materiałowych i geometrycznych jako zmienne losowe i wyznaczenie wartości oczekiwanych oraz odchyłeń standardowych naprężeń kontaktowych. Obliczenia numeryczne wykonano przy pomocy programu matematycznego do obliczeń symbolicznych MAPLE. Dzięki jego zastosowaniu wykonano wizualizację wybranych elementów losowych, a także gradientów wrażliwości naprężeń kontaktowych. Zaproponowane w pracy podejście można rozszerzyć na rozwiązania analityczne zagadnień kontaktowych o bardziej skomplikowanej geometrii, a także w odpowiednich implementacjach numerycznych Metody Elementów Skończonych lub Metody Elementów Brzegowych.

Manuscript received February 8, 2001; accepted for print April 27, 2001